Results in Physics 5 (2015) 92–98

Contents lists available at ScienceDirect

Results in Physics

journal homepage: www.journals.elsevier.com/results-in-physics

Heat transfer analysis of Rabinowitsch fluid flow due to metachronal wave of cilia

Noreen Sher Akbar, Adil Wahid Butt

DBS&H, CEME, National University of Sciences and Technology, Islamabad, Pakistan

ARTICLE INFO

Article history:
Received 27 February 2015
Accepted 20 March 2015
Available online 7 April 2015

Keywords:
Rabinowitsch fluid
Cilia motion
Exact solutions

ABSTRACT

The present investigation concerns with the mechanical properties of a Rabinowitsch fluid model and the effects of thermal conductivity over it. Flow is considered to be occurring due to metachronal wave produced as a result of constant beating of cilia at the walls of a horizontal circular tube. The expressions for flow characteristics have been derived results are analyzed graphically and discussed briefly.

Introduction

Rabinowitsch fluid lies in the category of pseudoplastic fluids (shear thinning fluids) such as blood. This model effectively describes the effects of lubricant additives and fits experimental data for a vast range of shear rate. During the past decades, tribologists have been efficiently putting their efforts to increase the efficiency of stabilizing properties of non-Newtonian lubricants by addition of small amounts of long chain polymer solutions. The use of additives minimizes the sensitivity of the lubricant to the change in the shearing strain rate. Further, the viscosity of these lubricants exhibits a non-linear relationship between the shearing stress and shearing strain rate. This model behaves as a Dilatant fluid for $\kappa < 0$, Newtonian fluid for $\kappa = 0$, and pseudoplastic fluid for $\kappa > 0$. The experimental verification for this Rabinowitsch fluid model was first given by Wada and Hayashi [1]. They found that the film pressure and load capacity for pseudoplastic lubricants were smaller than those for the Newtonian fluids. Afterwards, the theoretical study of bearing performance with non-Newtonian lubricants using different fluid models was done by Bourgin and Gay [2] on journal bearing. Later this model was studied for circular plates bearing, squeeze film between two plane annuli and on infinitely wide parallel rectangular plates by various authors [3–6]. Recently, Singh et al. [7–9] used the model of Rabinowitsch fluid and presented the dynamic analysis of hydrostatic thrust and squeeze film bearings. However, according to the author's knowledge, the theoretical study of incompressible laminar flow for Rabinowitsch fluid model in a circular tube of finite length taking into account that the inner walls of the tube are ciliated, has not been investigated yet. Cilia are tiny hairlike structures which are present in the human body and are responsible for the transport of various fluids by their constant movement which produces a metachronal wave along the direction of the fluid. Theoretical study on ciliated structures can be found in the literature [10–19].

In the present paper, the effects of heat transfer on a Rabinowitsch fluid model in a circular tube with ciliated walls have been investigated. In the absence of pseudoplasticity, the results are compared with the pre-established results of Newtonian lubricants and found in good agreement. The application of Rabinowitsch fluid model in peristalsis is very useful in physiology and biomedicine as it is involved in pumping of blood in heart/lung machines. Some applications of the related fluid flow model have also been discussed by other authors [20–30].

Formulation of the problem

Consider an incompressible Rabinowitsch fluid in a circular tube of finite length $\prime L\prime$. Flow occurs due to the metachronal wave which is produced due to collective beating of the cilia with constant speed $\prime c\prime$ along the walls of the tube whose inner surface is ciliated. The geometry of the problem is presented in the cylindrical coordinate system $(\bar{R}, \bar{Z})$ in which $\bar{Z}$-axis lies along the center line of the tube and $\bar{R}$ is orthogonal to it, defined as shown in Fig. 1.

The governing equations in the fixed frame for an incompressible fluid can be written as:

$$\frac{\partial \bar{U}}{\partial \bar{R}} + \frac{\bar{U}}{\bar{R}} + \frac{\partial \bar{W}}{\partial \bar{Z}} = 0, \tag{1}$$

E-mail address: adil.maths86@gmail.com (A.W. Butt)

http://dx.doi.org/10.1016/j.rinp.2015.03.005
2211-3797/

Nomenclature

ϵ	ratio w.r.t cilia length	a	radius of the tube
P	pressure	u, w	velocities
r	variable along the tube	z	variable normal to the tube
$\bar{\boldsymbol{\tau}}$	extra stress tensor	μ	fluid viscosity
λ	wave length	c	wave speed
β	wave number	b	wave amplitude
κ	coefficient of pseudoplasticity	B_r	Brickmann number
α	measure of the eccentricity		

$$\rho\left(\frac{\partial}{\partial\bar{t}}+\bar{U}\frac{\partial}{\partial\bar{R}}+\bar{W}\frac{\partial}{\partial\bar{Z}}\right)\bar{U}=-\frac{\partial\bar{P}}{\partial\bar{R}}-\frac{1}{\bar{R}}\frac{\partial}{\partial\bar{R}}(\bar{R}\bar{S}_{\bar{R}\bar{R}})-\frac{\partial}{\partial\bar{Z}}(\bar{S}_{\bar{R}\bar{Z}})-\frac{\bar{S}_{\bar{\theta}\bar{\theta}}}{\bar{R}}, \tag{2}$$

$$\rho\left(\frac{\partial}{\partial\bar{t}}+\bar{U}\frac{\partial}{\partial\bar{R}}+\bar{W}\frac{\partial}{\partial\bar{Z}}\right)\bar{W}=-\frac{\partial\bar{P}}{\partial\bar{Z}}+\frac{1}{\bar{R}}\frac{\partial}{\partial\bar{R}}(\bar{R}\bar{S}_{\bar{R}\bar{Z}})+\frac{\partial}{\partial\bar{Z}}(\bar{S}_{\bar{Z}\bar{Z}}), \tag{3}$$

$$\rho c_p\left(\frac{\partial}{\partial\bar{t}}+\bar{U}\frac{\partial}{\partial\bar{R}}+\bar{W}\frac{\partial}{\partial\bar{Z}}\right)\bar{T}=\bar{S}_{\bar{R}\bar{R}}\frac{\partial\bar{U}}{\partial\bar{R}}+\bar{S}_{\bar{R}\bar{Z}}\frac{\partial\bar{W}}{\partial\bar{R}}+\bar{S}_{\bar{Z}\bar{R}}\frac{\partial\bar{U}}{\partial\bar{Z}}+\bar{S}_{\bar{Z}\bar{Z}}\frac{\partial\bar{W}}{\partial\bar{Z}}+k\left(\frac{\partial^2\bar{T}}{\partial\bar{R}^2}+\frac{1}{\bar{R}}\frac{\partial\bar{T}}{\partial\bar{R}}+\frac{\partial^2\bar{T}}{\partial\bar{Z}^2}\right), \tag{4}$$

where $\bar{P}$ is the pressure and $\bar{U}, \bar{W}$ are the respective velocity components in the radial $\bar{R}$ and axial $\bar{Z}$ directions in the fixed frame respectively. $\bar{T}$ is the temperature, k denotes the thermal conductivity, ρ is the density and c_p is the specific heat at constant pressure. The extra stress tensor for the Rabinowitsch fluid model [1] is defined as:

$$\bar{S}_{\bar{R}\bar{Z}}+\bar{\kappa}(\bar{S}_{\bar{R}\bar{Z}})^3=\mu\frac{\partial\bar{W}}{\partial\bar{R}}, \tag{5}$$

where $\bar{\kappa}$ is the coefficient of pseudoplasticity. The envelops of the cilia tips can be expressed mathematically as [10]:

$$\bar{R}=\bar{H}=\bar{f}(\bar{Z},\bar{t})=a+a\epsilon\cos\left(\frac{2\pi}{\lambda}(\bar{Z}-c\bar{t})\right), \tag{6}$$

$$\bar{Z}=\bar{g}(\bar{Z},\bar{Z}_0,\bar{t})=a+a\epsilon\alpha\sin\left(\frac{2\pi}{\lambda}(\bar{Z}-c\bar{t})\right), \tag{7}$$

where a denotes the mean radius of the tube, ϵ is the non-dimensional measure with respect to the cilia length, λ and c are the wavelength and wave speed of the metachronal wave respectively. $\bar{Z}_0$ is the reference position of the particle and α is the measure of the eccentricity of the elliptical motion. If no slip condition is applied, then the velocities of the transporting fluid are just those caused by the cilia tips, which can be given as:

$$\bar{W}=\frac{\partial\bar{Z}}{\partial\bar{t}_{\bar{Z}_0}}=\frac{\partial\bar{g}}{\partial\bar{t}}+\frac{\partial\bar{g}}{\partial\bar{Z}}\frac{\partial\bar{Z}}{\partial\bar{t}}=\frac{\partial\bar{g}}{\partial\bar{t}}+\frac{\partial\bar{g}}{\partial\bar{Z}}\bar{W}, \tag{8}$$

$$\bar{U}=\frac{\partial\bar{R}}{\partial\bar{t}_{\bar{Z}_0}}=\frac{\partial\bar{f}}{\partial\bar{t}}+\frac{\partial\bar{f}}{\partial\bar{Z}}\frac{\partial\bar{Z}}{\partial\bar{t}}=\frac{\partial\bar{f}}{\partial\bar{t}}+\frac{\partial\bar{f}}{\partial\bar{Z}}\bar{W}, \tag{9}$$

By applying Eqs. (6) and (7) in Eqs. (8) and (9), we obtain:

$$\bar{W}=\frac{-\frac{2\pi}{\lambda}(\epsilon\alpha ac\cos(\frac{2\pi}{\lambda})(\bar{Z}-c\bar{t}))}{1-\frac{2\pi}{\lambda}(\epsilon\alpha a\cos(\frac{2\pi}{\lambda})(\bar{Z}-c\bar{t}))},$$

$$\bar{U}=\frac{\frac{2\pi}{\lambda}(\epsilon ac\sin(\frac{2\pi}{\lambda})(\bar{Z}-c\bar{t}))}{1-\frac{2\pi}{\lambda}(\epsilon\alpha a\cos(\frac{2\pi}{\lambda})(\bar{Z}-c\bar{t}))}.$$

In the fixed coordinates $(\bar{R},\bar{Z})$, the flow between the two tubes is unsteady. It becomes steady in a wave frame $(\bar{r},\bar{z})$ moving with the same speed as the wave moves in the $\bar{Z}$-direction. The transformations between the two frames are:

$$\bar{r}=\bar{R},\quad \bar{z}=\bar{Z}-c\bar{t},\quad \bar{u}=\bar{U},\quad \bar{w}=\bar{W}-c,\quad \bar{p}(\bar{z},\bar{r},\bar{t})=\bar{p}(\bar{Z},\bar{R},\bar{t}). \tag{10}$$

We introduce the following non-dimensional variables:

$$r=\frac{\bar{r}}{a},\quad z=\frac{\bar{z}}{\lambda},\quad w=\frac{\bar{w}}{c},\quad u=\frac{\lambda\bar{u}}{ac},\quad p=\frac{a^2\bar{p}}{c\lambda\mu},$$
$$\theta=\frac{(\bar{T}-\bar{T}_0)}{\bar{T}_0},\quad t=\frac{c\bar{t}}{\lambda},$$
$$\delta=\frac{a}{\lambda},\quad \mathrm{Pr}=\frac{\mu c_p}{k},\quad E_c=\frac{c^2}{c_pT_0},\quad B_r=E_c\mathrm{Pr},$$
$$\mathbf{S}_{ij}=\frac{a\bar{\mathbf{S}}_{ij}}{c\mu},\quad \kappa=\frac{\bar{\kappa}\mu^2c^2}{a^2}, \tag{11}$$

where Re, Pr and B_r are the Reynolds, Prandtl and Brikmann number respectively. With the help of Eqs. (10) and (11) and under the assumptions of long wavelength and low Reynolds number, Eqs. (1)–(5) take the following form:

$$\frac{\partial u}{\partial r}+\frac{u}{r}+\frac{\partial w}{\partial z}=0, \tag{12}$$

$$\frac{\partial p}{\partial r}=0, \tag{13}$$

$$\frac{dp}{dz}=\frac{1}{r}\frac{\partial}{\partial r}(rS_{rz}), \tag{14}$$

$$\frac{1}{r}\frac{\partial}{\partial r}\left(r\frac{\partial\theta}{\partial r}\right)=-B_rS_{rz}\frac{\partial w}{\partial r}, \tag{15}$$

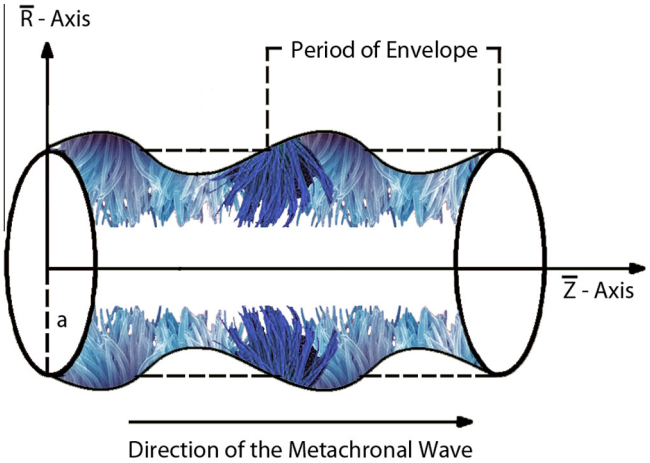

Fig. 1. Geometry of the problem.

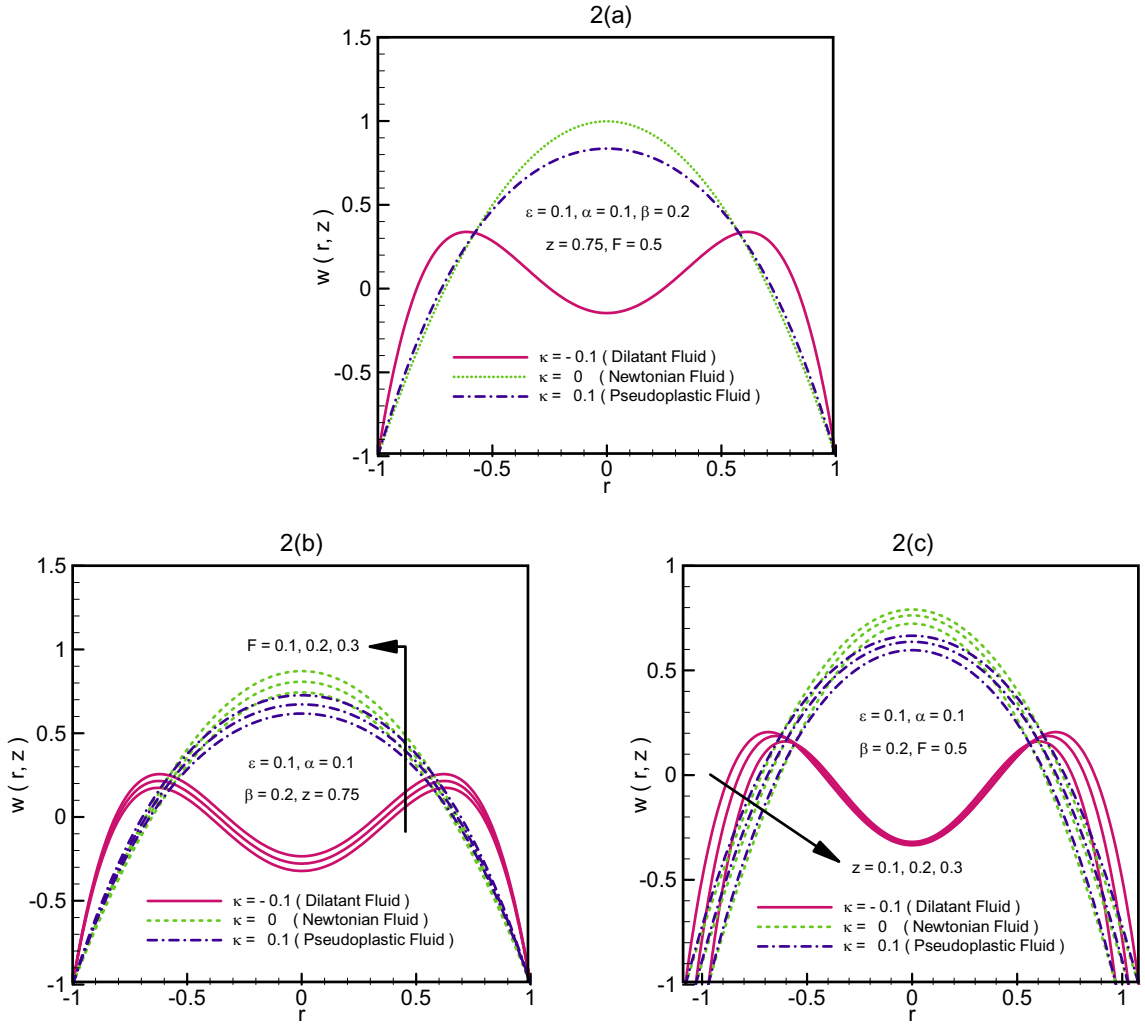

Fig. 2. Velocity profile $w(r,z)$ for different values of F and z.

$$S_{rz}+\kappa(S_{rz})^3=\frac{\partial w}{\partial r}. \tag{16}$$

The dimensionless form of the physical boundary conditions is:

$$w=\frac{-2\pi\epsilon\alpha\beta\cos(2\pi z)}{1-2\pi\epsilon\alpha\beta\cos(2\pi z)}-1,\quad \theta=0,\quad \text{at } r=h=1+\epsilon\cos(2\pi z), \tag{17}$$
$$\frac{\partial w}{\partial r}=0,\quad \frac{\partial\theta}{\partial r}=0,\quad \text{at } r=0.$$

Longitudinal momentum Eq. (14) subject to the boundary condition $S_{rz}=0$ at the symmetry line $r=0$, yields:

$$S_{rz}=\frac{r}{2}\frac{dp}{dz}. \tag{18}$$

Exact solutions

The exact solution of Eqs. 15 and 16 subject to the boundary conditions Eq. (17) is obtained as:

$$w(r,z)=\left(\frac{r^2-h^2}{4}\right)\frac{dp}{dz}+\kappa\frac{\left(r^4-h^4\right)}{32}\left(\frac{dp}{dz}\right)^3+\left(\frac{-2\pi\epsilon\alpha\beta\cos(2\pi z)}{2\pi\epsilon\alpha\beta\cos(2\pi z)-1}-1\right), \tag{19}$$

$$\theta(r,z)=\frac{1}{576}B_r\left(\frac{dp}{dz}\right)^2\left(\kappa\left(\frac{dp}{dz}\right)^2\left(h^6-r^6\right)+9\left(h^4-r^4\right)\right), \tag{20}$$

where $\frac{dp}{dz}$ can be found by using the volumetric flow flux:

$$Q=2\pi\int_0^h rw(r,z)dr.$$

An application of Eq. (19) and above Eq. yields:

$$Q=-\frac{1}{48}\pi h^2\left(h^4\kappa\left(\frac{dp}{dz}\right)^3+6h^2\frac{dp}{dz}-48\left(\frac{-2\pi\epsilon\alpha\beta\cos(2\pi z)}{1-2\pi\epsilon\alpha\beta\cos(2\pi z)}-1\right)\right). \tag{21}$$

The above equation is a 3rd order equation in $\frac{dp}{dz}$. To obtain the expression for pressure gradient, we find the real root to the above equation, which is as follows:

$$\frac{dp}{dz}=\frac{2^{\frac{1}{3}}\left(12B^2h^{12}\kappa^2A+\sqrt{2B^4h^{24}\kappa^3\left(\pi^2B^2h^6+72\kappa A^2\right)}\right)^{\frac{2}{3}}-(2\pi)^{\frac{2}{3}}B^2h^{10}\kappa}{\pi^{\frac{1}{3}}Bh^6\kappa\left(12B^2h^{12}\kappa^2A+\sqrt{2B^4h^{24}\kappa^3\left(\pi^2B^2h^6+72\kappa A^2\right)}\right)^{\frac{1}{3}}}, \tag{22}$$

where,

$$A=\left(\pi h^2-BQ\right),\quad B=(2\pi\epsilon\alpha\beta\cos(2\pi z)-1).$$

and the mean volume flow rate is defined as:

$$F=Q+\frac{1}{2}\left(1+\frac{\epsilon^2}{2}\right).$$

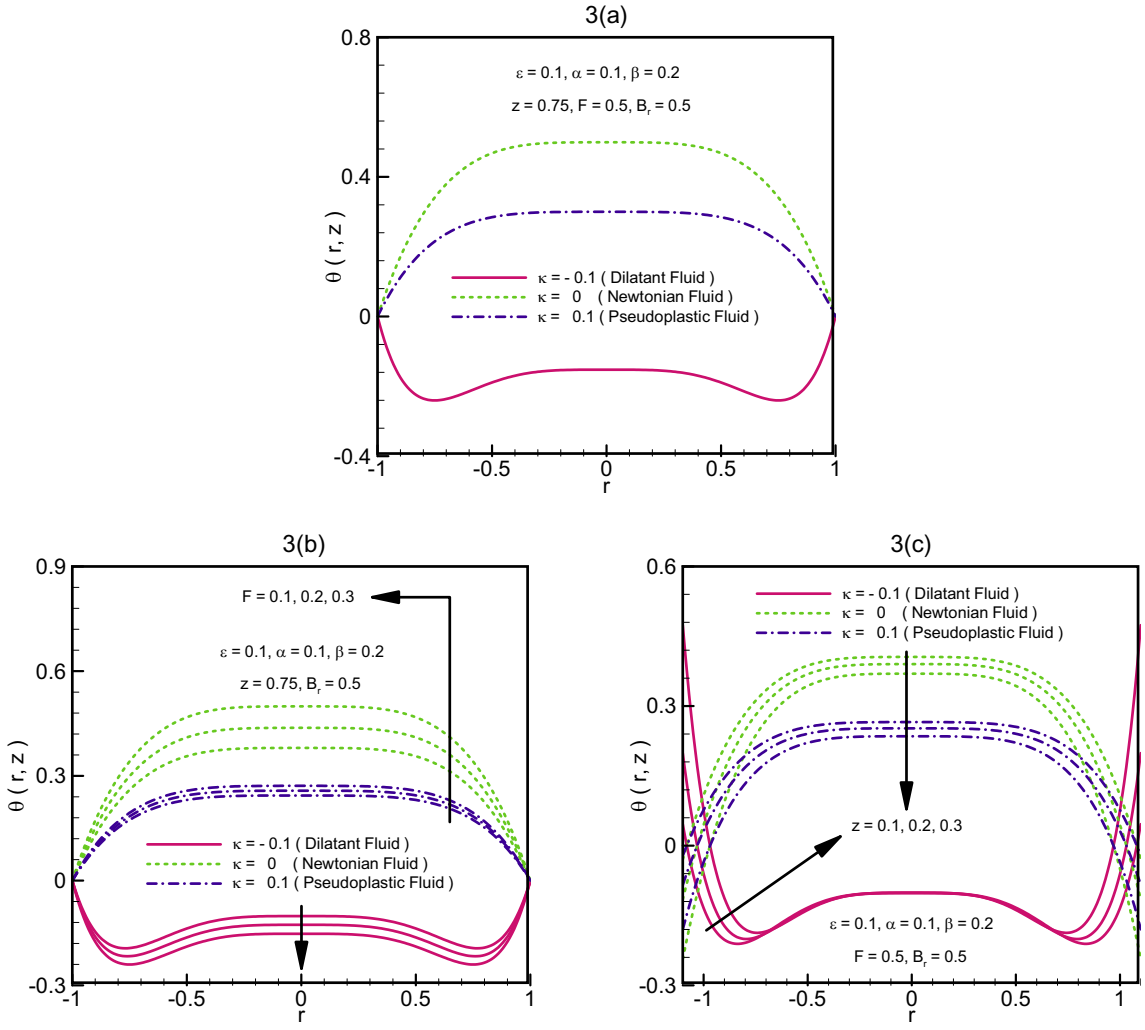

Fig. 3. Temperature profile $\theta(r,z)$ for different values of F and z.

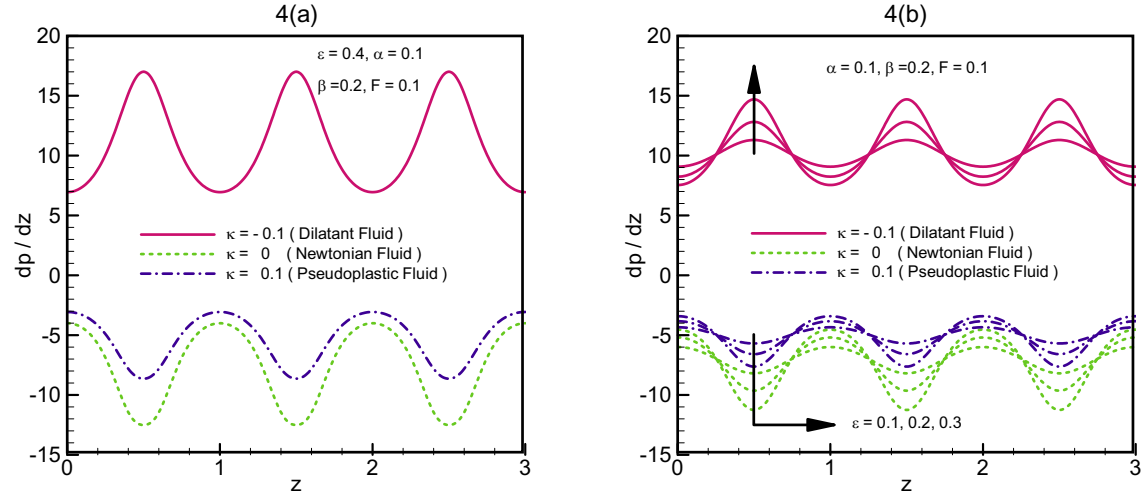

Fig. 4. Pressure gradient $\frac{dp}{dz}$ against the flow rate for different values of ϵ.

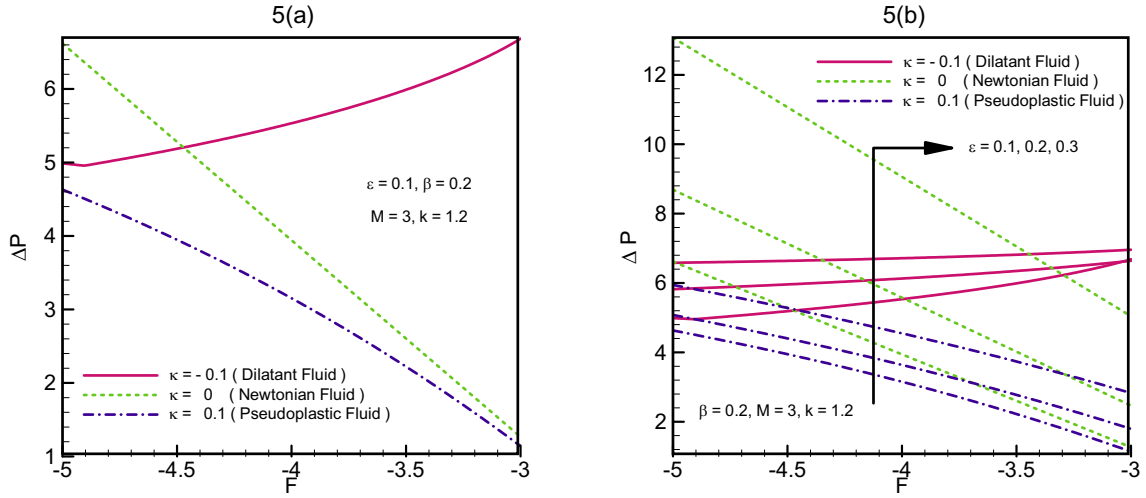

Fig. 5. Pressure gradient ΔP against the flow rate for different values of ϵ.

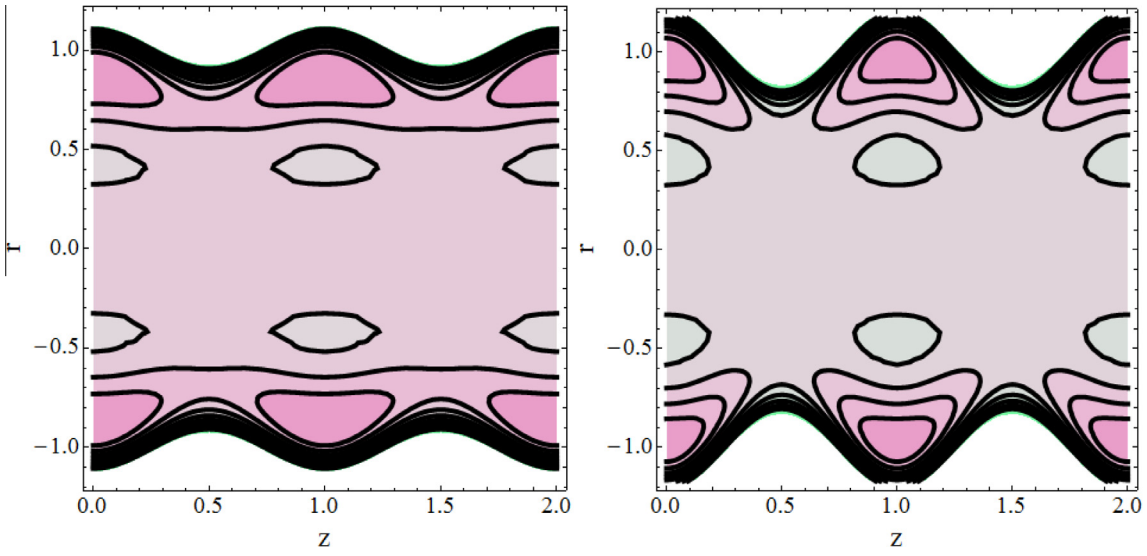

Fig. 6. Streamlines for velocity profile of Dilatant fluid $(\kappa < 0)$ for $\epsilon = 0.1, 0.2$, respectively.

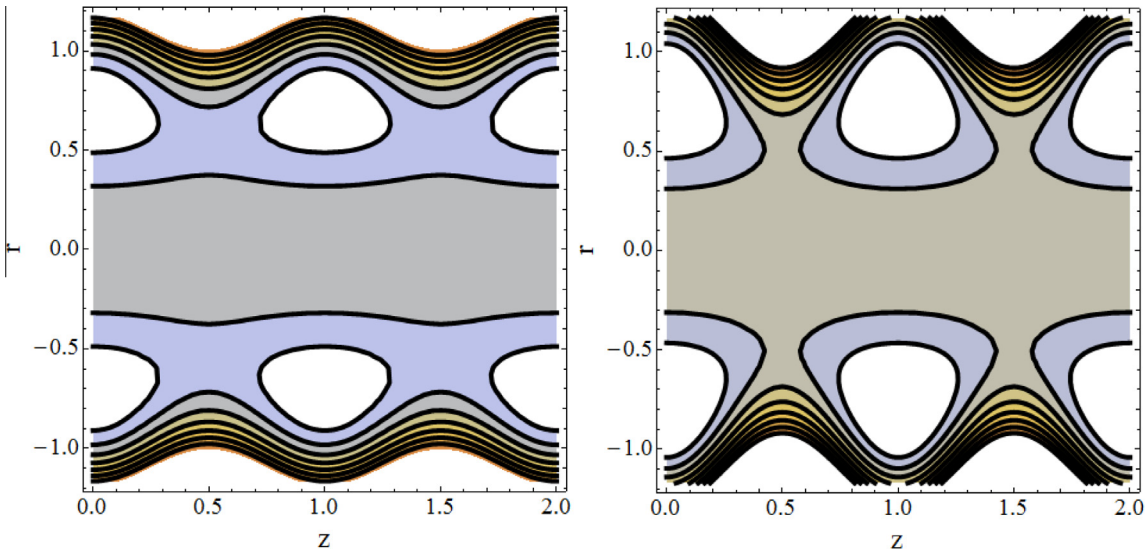

Fig. 7. Streamlines for velocity profile of Newtonian fluid $(\kappa = 0)$ for $\epsilon = 0.1, 0.2$, respectively.

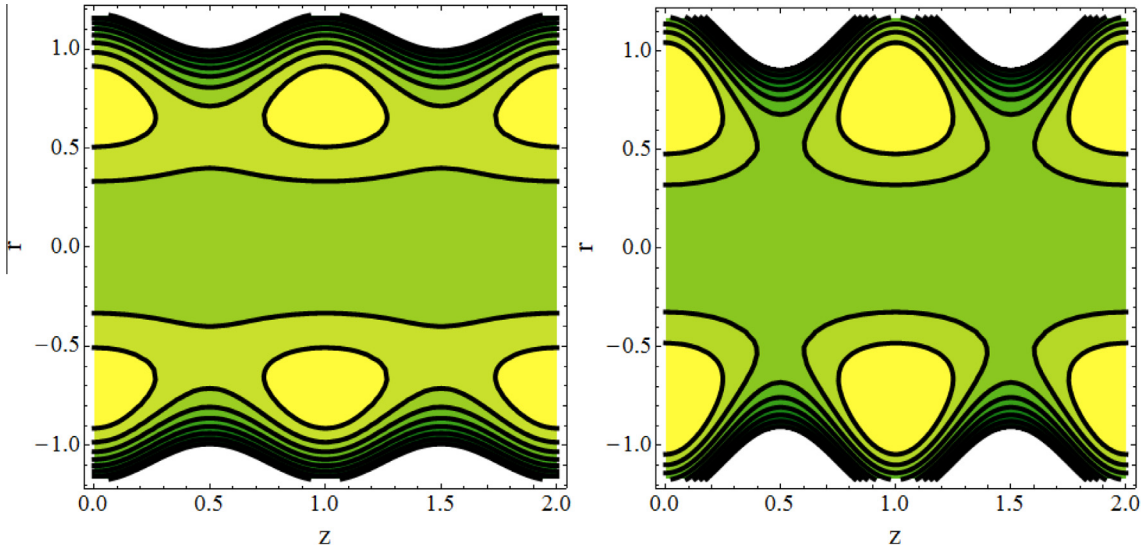

Fig. 8. Streamlines for velocity profile of Pseudoplastic fluid ($\kappa > 0$) for $\epsilon = 0.1, 0.2$, respectively.

The corresponding stream function can be found using the following formula:

$$w = \frac{1}{r}\frac{\partial \psi}{\partial r}.$$

The pressure rise ΔP is found by integrating the pressure gradient w.r.t z over the interval $[0, 1]$ as below:

$$\Delta P = \int_0^1 \frac{dp}{dz} dz.$$

Results and discussion

In order to present a quality analysis to the mechanical behavior of the concerned fluid flow and the effects of various parameters involved in it, exact solutions obtained in the previous section are presented here graphically. We have generated computer codes in Mathematica 9.0 to obtain the set of data files for velocity, temperature, pressure gradient and pressure rise, which are later used in Tecplot 10 to acquire the best pictorial representation.

Fig. 2(a–c) represents the effects of the coefficient of pseudoplasticity and the mean flow rate on the velocity of the fluid. It is observed that, in the center of the tube, the magnitude of dimensionless velocity is maximum for the Newtonian case and it increases with the Pseudoplasticity and decreases with the Dilatant nature of the fluid. Opposite behavior is seen at the walls of the tube where the flow is effected due to the metachronal wave of cilia. A similar behavior is observed with an increase in flow rate $|F|$, and decrease in the length of the tube.

The effect of flow rate over the coefficient of pseudoplasticity for the temperature profile is shown in Fig. 3(a–c). It is observed the temperature remains the same at the center of the tube for all values of $|\kappa|$, but it varies rapidly for the flow near the boundaries of the tube. Temperature increases at the walls for the Dilatant nature of the fluid, and it decreases more rapidly for Newtonian nature of the fluid as compared to the Pseudoplastic one. It is seen that as the mean flow rate increases, the temperature increases for Dilatant fluid but it decreases for both Newtonian and Pseudoplastic fluid. Temperature decreases for all types of fluid if we increase the length of the tube.

Fig. 4(a and b) shows the behavior of pressure gradient for non-dimensional measure with respect to the cilia length $|\epsilon|$. It is noticed that the pressure gradient has an oscillating behavior. For Dilatant fluid, the maximum values are attained at $z = 0.5, 1.5, 2.5\ldots$ for which we have the minimum values of both Newtonian and Pseudoplastic fluids. Similarly the relative minima of Dilatant fluid are attained at $z = 0, 1, 2, \ldots$ for which the relative maxima occur for Newtonian and Pseudoplastic fluids. Rapid change for values of Dilatant and Pseudoplastic fluid is seen as compared to the Newtonian nature of the fluid.

Pictorial representation of the pressure rise against the flow rate is given in Fig. 5(a–c). These graphs depict that an increase in the non-dimensional parameter $|\epsilon|$ causes an increase in the pressure rise. Trapping phenomenon is presented through Figs. 6–8 for Dilatant, Newtonian and Pseudoplastic nature of the present fluid model. It is seen that size of trapping bolus for Newtonian fluid is greater as compared to the Pseudoplastic and Dilatant fluid. It is also analyzed that when we extend the non-dimensional parameter $|\epsilon|$, the number of the trapped bolus increases but the size of trapped bolus decreases.

Conclusion

The effect of heat transfer on the flow of a Rabinowitsch fluid model through a circular tube with ciliated walls has been discussed. The magnitude of dimensionless velocity is maximum, at the center of the tube, for the Newtonian case and it increases with the Pseudoplasticity and decreases with the Dilatant nature of the fluid. Opposite behavior is seen at the walls of the tube. Increase in the mean flow rate $|F|$ causes an increase in the velocity. It is observed that the temperature remains the same at the center of the tube for all values of $|\kappa|$, but it varies rapidly for the flow near the boundaries of the tube. As the mean flow rate increases, the temperature increases for Dilatant fluid but it decreases for both Newtonian and Pseudoplastic fluid. It is observed that the pressure gradient has an oscillating behavior. For Dilatant fluid, the maximum values are attained at $z = 0.5, 1.5, 2.5\ldots$ for which we have the minimum values of both Newtonian and Pseudoplastic fluids. Similarly, the relative minima of Dilatant fluid are attained at $z = 0, 1, 2, \ldots$ for which the relative maxima occur for Newtonian and Pseudoplastic fluid. In the streamlines of the velocity profile, it is seen that size of trapping bolus for Newtonian fluid is greater as compared to the Pseudoplastic and Dilatant fluid. It is also analyzed that when we extend the non-dimensional parameter ϵ, the number of the trapped bolus increases but the size of trapped bolus decreases.

References

[1] Wada S, Hayashi H. Hydrodynamic lubrication of journal bearings by pseudoplastic lubricants. Bull JSME 1971;69:279–86.
[2] Bourgin P, Gay B. Determination of the load capacity of finite width journal bearing by finite element method in the case of a non-Newtonian lubricant. J Tribol 1984;106(2):285–90.
[3] Hsu YC, Saibel E. Slider bearing performance with a non-Newtonian lubricant. ASLE Trans 1965;8(2):191–4.
[4] Hashimoto H, Wada S. The effects of fluid inertia forces in parallel circular squeeze film bearing lubricated with pseudoplastic fluids. J Tribol Trans ASME 1986;108(2):282–7.
[5] Usha R, Vimla P. Fluid inertia effects in a non-Newtonian squeeze film between two plane annuli. J Tribol 1999;122:872–5.
[6] Hung CR. Effects of non-Newtonian cubic-stress flow on the characteristics of squeeze film between parallel plates. Educ Specialization 2009;97:87–97.
[7] Singh UP, Gupta RS, Kapur VK. On the steady performance of annular hydrostatic thrust bearing: Rabinowitsch fluid model. ASME J Tribol 2012;134:1341–5.
[8] Singh UP, Gupta RS, Kapur VK. On the performance of pivoted curved slider bearings: Rabinowitsch fluid model. Tribol Ind 2012;34:128–37.
[9] Singh UP. Application of Rabinowitsch fluid model to pivoted curved slider bearings. Arch Mech Eng 2013;LX:247–67.
[10] Sleigh MA. The biology of cilia and flagella. New York: MacMillian; 1962.
[11] Miller CE. An investigation of the movement of Newtonian liquids Initiated and sustained by the oscillation of Mechanical cilia. Aspen Emphysema Conf 1967:309–21.
[12] Blake JR. A spherical envelope approach to ciliary propulsion. J Fluid Mech 1971;46:199–208.
[13] Lardner TJ, Shack WJ. Cilia transport. Bull Math Biophys 1972;34:25–35.
[14] Blake JR. A model for the micro-structure in ciliated organisms. J Fluid Mech 1972;55:1–23.
[15] Sleigh MA, Aiello E. The movement of water by cilia. Acta Protozool 1972;11:265–77.
[16] Wu TY. Fluid mechanics of ciliary propulsion. In: Proceedings of the tenth anniversary meeting of the society of engineering science.
[17] Brennen C. An oscillating-boundary-layer theory for ciliary propulsion. J Fluid Mech 1974;65:799–824.
[18] Akbar NS, Butt AW, Noor NFM. Heat transfer analysis on transport of copper nanofluids due to metachronal waves of cilia. Curr Nanosci 2014;10(6):807–15.
[19] Akbar NS, Butt AW. CNT suspended nanofluid analysis in a flexible tube with ciliated walls. Eur Phys J Plus 2014;129:174.
[20] Vajravelu K, Sreenadh S, Ramesh Babu V. Peristaltic transport of a Herschel-Bulkley fluid in a an inclined tube. Int J Nonlinear Mech 2005;40:83–90.
[21] Hakeem AE, Naby AE, Misiery AEM, Shamy IE. Hydromagnetic flow of generalized Newtonian fluid through a uniform tube with peristalsis. Appl Math Comput 2006;173:856–71.
[22] Nadeem S, Akbar NS. Peristaltic flow of Sisko fluid in a uniform inclined tube. Acta Mech Sin 2010;26:675–83.
[23] Nadeem S, Akbar NS. Influence of heat and mass transfer on a peristaltic motion of a Jeffrey-six constant fluid in an annulus. Heat Mass Transfer 2010;46:485–93.
[24] Ellahi R, Rahman SU, Nadeem S. Theoretical study of unsteady blood flow of Jeffery fluid through stenosed arteries with permeable walls. Z Naturforsch A 2013;68a:489–98.
[25] Ellahi R, Riaz A, Nadeem S. Three dimensional peristaltic flow of Williamson in a rectangular duct. Indian J Phys 2013;87(12):1275–81.
[26] Nadeem S, Riaz A, Ellahi R, Akbar Noreen Sher. Series solution of unsteady peristaltic flow of a Carreau fluid in small intestines. Int J Biomath 2014;7(5):1450049.
[27] Ellahi R, Rahman SU, Nadeem S, Akbar Noreen Sher. Blood flow of nano fluid through an artery with composite stenosis and permeable walls. Appl Nanosci 2014;4:919–26.
[28] Nadeem S, Riaz A, Ellahi R, Akbar Noreen Sher. Mathematical model for the peristaltic flow of nanofluid through eccentric tubes comprising porous medium. Appl Nanosci 2014;4:733–43.
[29] Nadeem S, Sadaf H. Theoretical analysis of Cu-blood nanofluid for metachronal wave of cilia motion in a curved channel. Trans Nanobiosci 2015. http://dx.doi.org/10.1109/TNB.2015.2401972.
[30] Nadeem S, Sadaf H. Metachronal wave of cilia transport in a curved channel. Z Naturforsch A 2015;70:33–8.